Mound formation and slope selection in irreversible fcc (111) growth

Valery Borovikov* and Jacques G. Amar†
Department of Physics & Astronomy University of Toledo, Toledo, Ohio 43606, USA
(Received 7 June 2005; published 31 August 2005)

An analytic calculation of the surface current and selected mound angle is presented for the case of irreversible epitaxial growth on an fcc(111) surface with a finite Ehrlich-Schwoebel (ES) barrier. The special cases of short terraces and combinations of short terraces with facets which lead to large mound slopes are also discussed. We find that for both *A* and *B* steps the surface current and selected mound slope are determined by two key parameters—the Ehrlich-Schwoebel barrier and the degree of uphill funneling due to short-range attraction. However, the presence or absence of a small-slope instability is exclusively determined by the value of the ES barrier. In particular there exists a critical value of the parameter ρ (where $\rho=(\nu_{\mathrm{ES}}/\nu_0)e^{-E_{\mathrm{ES}}/k_BT}$ and E_{ES} is the ES barrier) such that for $\rho<\rho_c$, the flat surface is unstable to mound formation while for $\rho>\rho_c$ there is no such instability. The critical value $\rho_c\simeq 0.21$ is the same for both *A* and *B* steps and independent of the degree of uphill funneling due to short-range attraction. When the uphill funneling is not too large, the selected slope decreases continuously with increasing ρ, reaching zero at ρ_c. However, in the presence of sufficiently large uphill funneling, the selected slope is independent of ρ for $\rho<\rho_c$. In this case a new phenomenon which we refer to as fluctuation-induced instability also occurs. In particular, while the surface remains stable for $\rho>\rho_c$ for small slopes, for larger slopes the surface current may become positive due to uphill funneling. Thus, even in the presence of a small ES barrier, mound formation may still occur. Finally, we present typical results for the dependence of the mound slope on ρ for both *A* and *B* steps.

DOI: 10.1103/PhysRevB.72.085460 PACS number(s): 81.15.Aa, 68.55.−a, 68.43.Jk

I. INTRODUCTION

Recently there has been a great deal of interest in understanding the evolution of the surface morphology in epitaxial growth.[1] In particular, the formation of three-dimensional mound structures which grow and coarsen with increasing film thickness during homoepitaxial growth on singular (low-miscut) surfaces, has been observed in a wide variety of systems.[2–14] While in some cases mounds have been observed to form with a slowly increasing mound angle, in many cases, especially in metals, mounds have been observed to form with a clearly selected mound angle. Once formed, the typical mound size increases with increasing film thickness as mounds coalesce and coarsen to form new larger mound structures.

The origin of mound formation in homoepitaxial growth is the existence of a growth instability due to an uphill surface current. While a variety of different mechanisms, such as step-adatom attraction[15–17] or step-edge diffusion[18] may lead to such a current, in many cases the primary cause is the existence of a barrier to diffusion over descending steps, often called an Ehrlich-Schwoebel (ES) barrier.[19,20] In contrast, the "downward funneling" (DF)[21,22] of atoms deposited near steps typically leads to a stabilizing downhill surface current. The selection of a stable mound slope[23,24] is then determined by a balance between the uphill and downhill currents.

Recent molecular dynamics simulations[25,26] have shown that for epitaxial growth on metal (100) and (111) surfaces, the short-range attraction of depositing atoms to step edges can lead to significant deviations from the DF picture. In particular, short-range attraction can lead to significant "uphill funneling" for atoms deposited near step edges, thus decreasing the downhill current, enhancing the growth instability and increasing the selected mound angle. As a result, the selected mound slope depends not only on the strength of the ES barrier but also on the degree of "uphill funneling" due to short-range attraction.

For the case of irreversible growth on an fcc(100) surface, a general calculation of the surface current and selected mound slope as a function of the ES barrier and "degree of uphill funneling" has previously been carried out.[16,17] In addition, a general calculation of the surface current and selected mound slope which includes the effects of short-range attraction, has recently been carried out[26] for the case of arbitrary crystal geometry for the case of an infinite Ehrlich-Schwoebel barrier. Combined with the results of molecular dynamics simulations of the interaction of depositing atoms with step edges, such a calculation[26] has been used to estimate the selected mound slopes in Ag/Ag(111) and Cu/Cu(111) growth. However, there has been no calculation of the surface currents and selected mound slopes for fcc(111) surfaces for the more realistic case of a *finite* ES barrier. Such a calculation should be useful in obtaining a general understanding of the dependence of the selected mound slope and mound morphology on growth temperature and ES barrier in growth on fcc(111) surfaces.

Here we present the results of an analytic calculation of the surface current and selected mound slope as a function of the ES step barrier for the case of irreversible growth on fcc(111) surfaces. Our calculation also takes into account the effects of deviations from the standard downward funneling picture including the effects of short-range attraction as well as "knockout" for atoms deposited near step edges. We also consider the case in which the selected mound slope is larger than that corresponding to the narrowest "general" terrace width, and thus corresponds to a mixture of facets and terraces. This both corrects previous "large-slope" results obtained for the case of an infinite ES barrier[26] and generalizes them to account for the existence of a finite barrier. These

results are particularly important since experimentally the mound slope can be quite large, due to the combination of a reasonably large ES barrier and significant "uphill funneling" due to short-range attraction. Since there are two types of close-packed step edges on the fcc(111) surface: *A* steps corresponding to (100) microfacets and *B* steps corresponding to (111) microfacets, our calculations are carried out for both *A* and *B* steps.

We note that since our calculation assumes irreversible growth at step edges (i.e., no detachment) it applies at temperatures which are not too high such that detachment from steps can be neglected. In addition, it is based on the reasonable assumption that atoms on a flat fcc(111) terrace diffuse via nearest-neighbor hops between fcc and hcp sites. Due to the symmetry of the honeycomb lattice, our results are not affected by differences between the binding energies at fcc and hcp sites.

Before presenting the details of our calculations we first briefly summarize some of our main results. We find that for both *A* and *B* steps there are two key parameters—the ES barrier and the degree of uphill funneling due to short-range attraction—which determine the surface current and selected mound slope. While both parameters determine the value of the selected mound slope in the case of an instability, the presence or absence of a small-slope instability is exclusively determined by the ES barrier. In particular we find that for both *A* and *B* steps there exists a critical value of the Ehrlich-Schwoebel parameter $\rho=(\nu_{\mathrm{ES}}/\nu_0)e^{-E_{\mathrm{ES}}/k_BT}$ corresponding to $\rho_c \simeq 0.21$, such that for $\rho<\rho_c$, the surface is unstable to mound formation while for $\rho>\rho_c$ there is no instability. This result is qualitatively similar to that previously obtained[16] for the case of growth on fcc(100) surfaces. However, we also find that in the presence of sufficiently large uphill funneling, a new phenomenon which we refer to as fluctuation-induced instability occurs. In this case, while the surface is stable for small slopes, for large slopes the surface current becomes positive. Thus, mound formation may still occur for $\rho>\rho_c$ if fluctuations (due, for example, to deposition noise) are sufficiently large for the local slope to exceed the instability threshold. This is a feature which has not been previously discussed and which occurs in the presence of a large uphill funneling probability. We also find that for large uphill funneling the selected slope is independent of ρ for $\rho<\rho_c$. Finally, we note that while the expressions for the surface current of *A* and *B* steps are, in general, quite similar, due to differences in the uphill funneling probabilities at *A* and *B* steps, our results indicate that there is, in general, a strong asymmetry in the mound shape.

The paper is organized as follows. In Sec. II we describe our model. In Sec. III, we describe the calculation of the surface current and selected mound slope for both *A* and *B* steps. The cases of short terrace lengths and mixture of terraces with different lengths are discussed separately. In Sec. IV we analyze and discuss our results. Finally, in Sec. V we summarize our results.

II. MODEL

To calculate the surface current, we consider a regular stepped fcc(111) surface with infinitely long straight steps

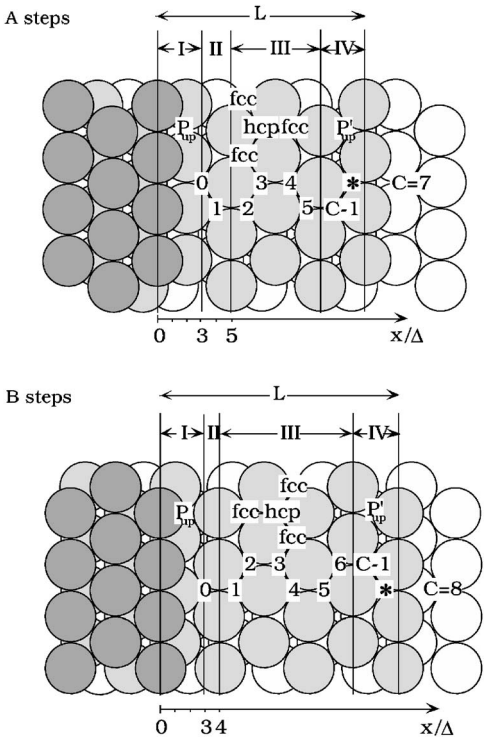

FIG. 1. Schematic diagram (top view) of *A* and *B* steps on fcc(111) surface. Site labeled * corresponds to the last threefold hollow site on the upper terrace (see text).

(either *A* or *B* steps, see Fig. 1) and terrace width *L*. As shown in Fig. 1, the total surface current per particle J/F, where J is the surface current and F is the deposition flux, may be divided into four contributions due to deposition in four different regions. Region I corresponds to atoms deposited just beyond the step edge but close enough to feel the effects of short-range attraction to the step. Region II corresponds to the particles that land slightly farther away from the step edge and is needed to connect to the terrace region. Region III corresponds to atoms deposited on a terrace away from a step. Finally region IV corresponds to atoms deposited near a step edge on the upper side. In region III we apply a discrete approach, while in regions I, II, and IV we apply a continuous approach. To fix our notation, for convenience, we define $\Delta=\sqrt{3}a_1/6$ as the unit of length, where a_1 is the nearest-neighbor distance. The selected terrace width L_0 and corresponding selected slope $m_0=h/L_0$ (where the layer height $h=\sqrt{6}a_1/3$) then correspond to those values for which the surface current per particle J/F is equal to zero. Taking into account that the unit of length was defined as $\Delta=\sqrt{3}a_1/6$, the selected slope m_0 may be written as $m_0=2\sqrt{2}/L_0$. In our units, regions I and IV are of width 3 while the bridge region II is of width 2 (1), and the terrace region III is of width $L-8$ $(L-7)$ for $A(B)$ steps. This implies that the minimum "general" terrace width is given by $L=8$ $(L=7)$ for $A(B)$ steps.

For a given terrace length *L*, the surface current per particle may be calculated[16] by multiplying the probability that an atom will be deposited at a given site by the average (signed) distance traveled before absorption at an ascending or descending step.[33] For simplicity, we assume irreversible

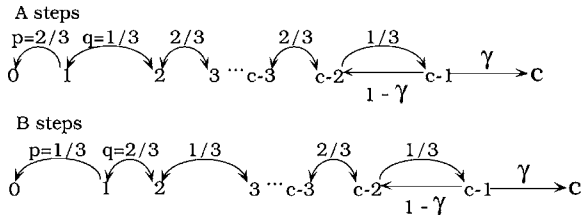

FIG. 2. Diagram showing random walk between absorbing sites at 0 and c. γ corresponds to overall probability that at an atom at site $c-1$ will diffuse to the layer below (see text).

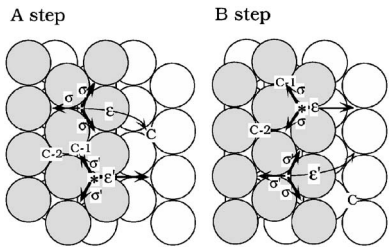

FIG. 3. Diagram showing details of interlayer diffusion at A and B steps.

attachment at ascending steps (sites 0 or c in Fig. 1) which is appropriate for a variety of systems over a range of temperatures, although at high temperatures detachment from step edges may need to be taken into account. Atoms which are deposited on a flat terrace away from a step edge are assumed to first "cascade" to the nearest fcc or hcp site and then hop alternately between fcc and hcp sites until reaching the fcc attachment site at an ascending step edge (see Fig. 1). We note that very recent work[27] indicates that for some systems, single-atom diffusion may occur via correlated long jumps above a critical system-dependent temperature. However, here we assume that we are at low enough temperatures that such correlated jumps do not occur.

We note that while there exists a difference between the binding energies of adatoms at fcc and hcp sites,[28] this difference does not affect the results of our calculations. For example, if an atom is at a fcc (hcp) hollow site on a flat terrace away from a step edge, it can hop with *equal* probability to each one of the three nearest hcp (fcc) sites (see Fig. 1). Accordingly, the probability of an atom to hop away (towards) the ascending step alternates between the values of $1/3$ and $2/3$ depending on whether or not the adatom is at an fcc or an hcp site on the terrace. As a result, the diffusion process can be mapped to a one-dimensional random walk with alternating probabilites p and $q=1-p$ between two absorbing barriers, one at site 0 corresponding to the ascending step-edge and the other at site c corresponding to the descending step (see Fig. 2). For example, if an atom is at site k, and k is odd, the probability of hopping to site $k-1$ is given by p, where $p=1/3$ $(2/3)$ for A steps (B steps), while the probability of hopping to site $k+1$ is given by $q=1-p$. Similarly, if k is even, the probability of hopping to site $k-1$ $(k+1)$ is given by q $(p=1-q)$.

Due to the existence of the Ehrlich-Schwoebel step-barrier,[19,20] the rate for an atom at the edge of a step to diffuse to the terrace below is typically different from the rate for hopping on a flat terrace. For generality we assume that adatoms may hop/exchange to the terrace below from both the fcc and hcp sites closest to the step edge. In particular, we assume (see Fig. 3) that for an atom in the last fcc site closest to the step edge, the probability to go over the step (either via hopping or exchange) to the absorption site c is given by ϵ, where the value of ϵ is in general different for A and B steps. Similarly, the corresponding probabilities for interlayer diffusion from the hcp site closest to the step edge are given by ϵ'. We note that for A steps the site closest to the step edge is an hcp site, while for B steps it is an fcc site. We also note that in Figs. 1 and 3 the last threefold hollow site on the top terrace (site *) is not numbered even though atoms can hop from site $c-1$ to this site. The reason is that, as explained in more detail below and in the Appendix, one can combine the probabilities for an atom to diffuse to the lower step—either directly from site $c-1$ or after hopping from site $c-1$ to site *—into a single overall probability γ for an atom at site $c-1$ to diffuse to the layer below. In order to calculate the surface current J, we also need to take into account the effects of short-range attraction[16,17,25,26] of atoms deposited near step edges and the effects of "knockout" of step-edge atoms,[29] as we discuss in more detail below.

III. SURFACE CURRENT AND SELECTED MOUND SLOPE

A. General expression for attachment probabilities P_i

Before calculating the surface current, we first obtain general expressions for the absorption probability P_i that a particle at site i on a terrace will attach to the ascending step (see Fig. 1). The solution to this problem is equivalent (see Appendix) to the solution of a simpler problem corresponding to a random walk between two absorbing sites 0 and c in which the particle hops directly from the last site $c-1$ to absorbing site c with probability γ, and from $c-1$ to site $c-2$ with probability $1-\gamma$ while the probability of hopping on a flat terrace away from a step-edge alternates between the values p and $q=1-p$. As shown in the Appendix, one may map the process of interlayer diffusion from the fcc and hcp sites closest to the step edge (site $c-1$ and the last site on the terrace, see Fig. 3), where ϵ and ϵ' are the corresponding probabilities of interlayer diffusion, to a simplified problem in which the overall probability that an atom at site $c-1$ arrives at the lower terrace (either directly from site $c-1$ or after passing through the last site on the terrace) is given by $\gamma(\epsilon,\epsilon')$, where the expression for $\gamma(\epsilon,\epsilon')$ is different for A and B steps. The probability P_i of absorption at site 0 may then be found by solving the following set of difference equations for this simplified problem[30]

$$P_{2k-1} = pP_{2k-2} + qP_{2k}, \quad 1 \leqslant k \leqslant \frac{c-1}{2}, \tag{1a}$$

$$P_{2k} = qP_{2k-1} + pP_{2k+1}, \quad 1 \leqslant k \leqslant \frac{c-3}{2}, \tag{1b}$$

$$P_{c-1} = (1-\gamma)P_{c-2} + \gamma P_c, \tag{1c}$$

where $p=2/3$ $(1/3)$ for A (B) steps with boundary conditions $P_0=1$ and $P_c=0$.

For odd c corresponding to A steps (where $c=2K+3$ and $K=0, 1, 2,\ldots$) the solution is given by[30]

$$P_{2k} = 1 - \frac{k}{K+q+(p/\gamma)}, \quad 0 \leqslant k \leqslant \frac{c-3}{2}, \tag{2a}$$

$$P_{2k+1} = 1 - \frac{k+q}{K+q+(p/\gamma)}, \quad 0 \leqslant k \leqslant \frac{c-3}{2}, \tag{2b}$$

$$P_{c-1} = 1 - \frac{K+1}{K+q+(p/\gamma)}, \tag{2c}$$

where $K=(c-3)/2$. For even c corresponding to B steps (where $c=2K+2$ and $K=0, 1, 2,\ldots$) the solution is given by

$$P_{2k} = 1 - \frac{k}{K+(q/\gamma)}, \quad 0 \leqslant k \leqslant \frac{c-2}{2}, \tag{3a}$$

$$P_{2k+1} = 1 - \frac{k+q}{K+(q/\gamma)}, \quad 0 \leqslant k < \frac{c-2}{2}, \tag{3b}$$

$$P_{c-1} = 1 - \frac{K+q}{K+(q/\gamma)}, \tag{3c}$$

where $K=(c-2)/2$.

B. Surface current for A steps ($L \geqslant 8$)

We first consider the surface current for the case of A steps with terrace width $L \geqslant 8$. In this case $p=\frac{2}{3}$ while the relationship between the absorption site c in the 1D random-walk picture (Fig. 2) and the terrace width L in our units is $L=(3c+7)/2$, where c is an integer which satisfies $c=2K+3$, where $K=0, 1, 2, 3,\ldots$. As shown in Fig. 1, the total surface current per particle J/F, may be divided into four contributions due to deposition in four different regions. We first consider the contribution J_3/F due to atoms deposited in region III away from the step edges. Since this region is far away from the steps, an atom deposited in this region will first arrive at either the nearest fcc or hcp site. If an atom is deposited at an even (fcc) site $2k$, the probability of absorption at site 0 is given by P_{2k} while the distance between the deposition site and the attachment site is $d_{2k}=3k$. However, if an atom is deposited at an odd (hcp) site $2k+1$, the probability of absorption at site 0 is given by P_{2k+1} while the distance between the deposition site and attachment site is given by $d_{2k+1}=3k+1$. This leads to the following expression for the surface current per particle:

$$\frac{J_3}{F} = \frac{3}{2L}\left\{\sum_{k=1}^{K}[3kP_{2k} - (L-3k)(1-P_{2k})] + \sum_{k=1}^{K}[(3k+1)P_{2k+1} - (L-3k-1)(1-P_{2k+1})]\right\}, \tag{4}$$

where the first summation corresponds to even sites and the second summation to odd sites. The first (second) term in each of the summations corresponds to the product of the signed distance a particle must travel from the initial landing position to the absorption site at an ascending (descending) step times the probability of arriving at that site. The factor of $1/L$ corresponds to the deposition probability per unit interval Δ while the factor of $\frac{3}{2}$ is a normalization factor which takes into account the fact that in the sum we have included *two* sites per *three* units of length Δ in discrete region III. Taking into account that $L=(3c+7)/2$ and $c=2K+3$ for A steps, we obtain

$$K = \frac{L-8}{3}. \tag{5}$$

Substituting Eqs. (2a)–(2c) for P_i along with Eq. (5) for K into Eq. (4) and using the well-known formula for arithmetic series, we obtain for the surface current in region III

$$\frac{J_3}{F} = \frac{(2-7\gamma)(32-12L+L^2)}{2L[2+\gamma(L-7)]}, \tag{6}$$

where $\gamma=(3\epsilon+2\epsilon'-2\epsilon\epsilon')/(1+2\epsilon+2\epsilon'-2\epsilon\epsilon')$ (see Appendix).

The second contribution to the surface current corresponds to atoms deposited within a distance $\delta=\pm 3\Delta$ from the step edge (regions I and IV, see Fig. 1). We first discuss region I corresponding to atoms deposited beyond the step edge. To take into account the effects of short-range attraction during deposition, we consider the local uphill funneling probability $P^A(x)dx$ that an atom deposited above the *lower* terrace at an initial distance between x and $x+dx$ beyond the step edge lands on the *upper* terrace (see Fig. 1). We assume that upon landing such an atom "cascades" to the last terrace site (site *) with probability $\alpha(x)$ and to the next-to-last terrace site (site $c-1$) with probability $\beta(x)$, where $\alpha(x)+\beta(x)=1$. This leads to the following expression for the corresponding surface current:

$$\begin{aligned}\frac{J_1}{F} = {} & \frac{1}{L}\int_L^{L+3}[\alpha(x)(1-\epsilon')P_{c-1} + \beta(x)P_{c-1}]P^A(x)(x-3)dx \\ & - \frac{1}{L}\int_L^{L+3}\alpha(x)[\epsilon' + (1-\epsilon')(1-P_{c-1})] \\ & \times P^A(x)(L+3-x)dx \\ & - \frac{1}{L}\int_L^{L+3}\beta(x)(1-P_{c-1})P^A(x)(L+3-x)dx \\ & - \frac{1}{L}\int_L^{L+3}[1-P^A(x)](L+3-x)dx.\end{aligned} \tag{7}$$

The first integral corresponds to atoms which land on the upper terrace and then diffuse to the ascending step's attachment site. (The second term corresponds to atoms which land directly on site $c-1$ while the first term corresponds to atoms which first land on the last terrace site and then hop to site $c-1$ with probability $1-\epsilon'$.) Similarly, the second and third integrals correspond to atoms which land on the upper terrace and then diffuse to the descending step's attachment site. The fourth integral corresponds to atoms which land on the lower terrace after being deposited and then attach immediately (without diffusing) to the descending step. The

factor of $1/L$ arises from the fact that the probability that the particle lands in a particular interval dx is given by dx/L.

Similarly, in region IV, we consider the local uphill funneling probability $P'^A(x)dx$ that an atom deposited above the *upper* terrace at an initial distance between x and $x+dx$ from a step edge lands on the *upper* terrace (see Fig. 1). We assume that upon landing such an atom arrives at the last terrace site (next-to-last terrace site $c-1$) site with probability $\alpha'(x)$ $[\beta'(x)]$, where $\alpha'(x)+\beta'(x)=1$. This leads to the following expression for the corresponding surface current:

$$\begin{aligned}\frac{J_4}{F} &= \frac{1}{L}\int_{L-3}^{L}[\alpha'(x)(1-\epsilon')P_{c-1}+\beta'(x)P_{c-1}]P'^A(x)(x-3)dx \\ &- \frac{1}{L}\int_{L-3}^{L}\alpha'(x)[\epsilon'+(1-\epsilon')(1-P_{c-1})] \\ &\times P'^A(x)(L+3-x)dx \\ &- \frac{1}{L}\int_{L-3}^{L}\beta'(x)(1-P_{c-1})P'^A(x)(L+3-x)dx \\ &- \frac{1}{L}\int_{L-3}^{L}[1-P'^A(x)](L+3-x)dx. \end{aligned} \tag{8}$$

Except for the range of integration and the uphill funneling probabilities, the explanation of the integrals is the same as for region I [Eq. (7)].

Combining both contributions, we obtain an expression for the contribution from regions I and IV,

$$\frac{J_1+J_4}{F} = \frac{6[P'^A_\alpha+P^A_\alpha+P'^A_\beta+P^A_\beta-\epsilon'(P'^A_\alpha+P^A_\alpha)](1-\gamma)}{2+\gamma(L-7)} - \frac{18}{L}, \tag{9}$$

where we have introduced the quantities

$$P'^A_\alpha = \frac{1}{3}\int_{L-3}^{L}\alpha'(x)P'^A(x)dx, \tag{10a}$$

$$P^A_\alpha = \frac{1}{3}\int_{L}^{L+3}\alpha(x)P^A(x)dx, \tag{10b}$$

$$P'^A_\beta = \frac{1}{3}\int_{L-3}^{L}\beta'(x)P'^A(x)dx, \tag{10c}$$

$$P^A_\beta = \frac{1}{3}\int_{L}^{L+3}\beta(x)P^A(x)dx \tag{10d}$$

corresponding to the overall probabilities $(P'^A_\alpha, P^A_\alpha)$ $[(P'^A_\beta, P^A_\beta)]$ that an atom uniformly deposited in regions I or IV remains on the upper terrace at the last (next-to-last) site immediately after deposition.

Finally, we consider the contribution from the "buffer" region II which can be simply expressed as

$$\begin{aligned}\frac{J_2}{F} &= \frac{1}{L}\int_3^5\left[\frac{1}{3}(x-3)+\frac{2}{3}[P_1(x-3)-(1-P_1)(L-x+3)]\right]dx \\ &= \frac{2[6+\gamma(L-21)]}{3L[2+\gamma(L-7)]}. \end{aligned} \tag{11}$$

Here we have taken into account that an atom deposited in region II arrives without diffusion at site 0 with probability $\frac{1}{3}$, while the probability of arriving at site 1 is $\frac{2}{3}$. From site 1 the atom can diffuse to the ascending-step attachment site 0 with probability P_1, or to the lower-terrace attachment site c with probability $1-P_1$.

Making two reasonable assumptions, we can simplify the expressions that include uphill funneling probabilities. The first assumption is that $P'^A_\alpha = P'^A_\beta = \frac{1}{2}P'^A_{up}$. This is consistent with the fact that deposition in region IV is equally likely to be above the last fcc site as above the last hcp site and is also consistent with the results of recent molecular dynamics simulations carried out for deposition near A steps on Cu(111) and Ag(111).[26] The second assumption is that atoms deposited beyond an A-step edge will arrive at the nearest threefold hollow site, i.e., $P^A_\alpha = P^A_{\rm up}$ and $P^A_\beta = 0$. Using these assumptions, combining all four contributions and using the expression $\gamma=(3\epsilon+2\epsilon'-2\epsilon\epsilon')/(1+2\epsilon+2\epsilon'-2\epsilon\epsilon')$ derived in the Appendix, we obtain the following general expression for the total surface current for a periodic sequence of terraces of width L separated by A steps:

$$\frac{J^A}{F} = \frac{(6-51\epsilon-30\epsilon'+30\epsilon\,\epsilon')L-72(1-P^A_{\rm av})}{D_A} + \frac{\epsilon'[152-18(P'^A_{\rm up}+2P^A_{\rm up})]+\epsilon(300-72P^A_{\rm av})-\epsilon\,\epsilon'[152-18(P'^A_{up}+2P^A_{\rm up})]}{D_A}, \tag{12}$$

where $L \geqslant 8$, $P'^A_{\rm up} = P'^A_\alpha + P'^A_\beta$, $P^A_{\rm up} = P^A_\alpha + P^A_\beta$, $P^A_{\rm av} = (P'^A_{\rm up} + P^A_{\rm up})/2$ and $D_A = (18\epsilon+12\epsilon'-12\epsilon\,\epsilon')L+12-102\epsilon-60\epsilon'+60\epsilon\,\epsilon'$.

We note that Eq. (12) is valid for arbitrary probabilities ϵ and ϵ' of interlayer diffusion from the last fcc and hcp sites as well as for arbitrary mechanisms (e.g., exchange or hopping) of interlayer diffusion. On the other hand, recent *ab initio* calculations for Pt(111) A and B steps,[28] indicate that the dominant diffusion mechanism responsible for downward transport over both A and B steps on fcc(111) metal surfaces is the exchange mechanism. If we consider the details of such an exchange process for the case of Pt(111),[28] we note

that during the exchange the diffusing adatom first moves from an initial fcc site near the step edge to a saddle position which is symmetrically located between the last fcc and hcp sites. From this position it then "pushes" the nearest step atom towards the absorption site on the lower terrace, taking its place. This indicates that the processes of exchange from the last fcc site (site $c-1$) and from the last (hcp) terrace site should be almost equivalent. Thus, if we define the binding-energy difference between an fcc site and an hcp site along the step by δE_b then the rate of hopping from the last hcp site to any of the nearby fcc sites is $e^{\delta E_b/k_BT}$ times greater than the rate of hopping from the last fcc site to any of the nearby hcp sites. However, the barrier for exchange at a step edge is correspondingly reduced by δE_b for the hcp site compared to the fcc site. As a result, the difference in the binding energy between fcc and hcp sites effectively cancels out. Using this fact, we can see that the probabilities ϵ and ϵ' for interlayer diffusion from the last fcc and hcp sites, respectively, depend only on the ES parameter $\rho=(\nu_{\mathrm{ES}}/\nu_0)\exp(-E^A_{\mathrm{ES}}/k_BT)$ where E^A_{ES} corresponds to the ES barrier for exchange from the last fcc site and ν_{ES}/ν_0 is the ratio of prefactors for exchange versus terrace diffusion. In particular (see Appendix), we find $\epsilon=\rho/(3+\rho)$ and $\epsilon'=\rho/(2+\rho)$. Using these expressions for ϵ and ϵ' in Eq. (12), we obtain

$$\frac{J^A}{F}=\frac{3(4-18\rho-5\rho^2)L-144(1-P^A_{\mathrm{av}})+2(116+9P'^A_{\mathrm{up}})\rho+76\rho^2}{6[4+(4L-18)\rho+(L-5)\rho^2]}, \tag{13}$$

where $L\geqslant 8$. From Eq. (13) we may obtain the selected slope $m^A_0=h/L_0=2\sqrt{2}/L_0$, corresponding to the value of the terrace length for which the surface current J/F is zero:[23,24]

$$m^A_0=\frac{3\sqrt{2}(4-18\rho-5\rho^2)}{72(1-P^A_{\mathrm{av}})-(116+9P'^A_{up})\rho-38\rho^2}\left(m^A_0\leqslant\frac{\sqrt{2}}{4}\right). \tag{14}$$

As already noted, expressions (13) and (14) are only correct for terrace length $L\geqslant 8$ which corresponds to selected slopes $m_0\leqslant\sqrt{2}/4$, since for higher slopes (smaller terrace widths) there is an overlap between the regions II and IV.

C. Surface current for A steps ($L=5$)

We now consider the surface current for the special case of shorter terrace lengths $L<8$ for which there is an overlap between regions II and IV and, as a result, Eqs. (13) and (14) may break down. Since the possible terrace widths for A steps are $L=2, 5, 8\ldots$, the two possible special cases correspond to $L=2$ and $L=5$. The first case ($L=2$) corresponds to a (100) microfacet for which the surface current is negative in our model. So we only need to consider the special case $L=5$.

In this case the only sites on the terrace (see Fig. 4) where deposited atoms can land correspond to the absorption fcc site 0 and hcp site 1. We consider the contributions to the surface current from two regions: region I ($5\leqslant x<7.5$) and region IV ($2.5\leqslant x<5$), which are similar to but slightly different from the regions I and IV considered in the general case. We assume that there is no diffusion down the step from these sites due to bonding to the ascending step edge. Consequently, $P_1=P_0=1$. The resulting expressions for the surface current have the following forms:

$$\frac{\tilde{J}_1}{F}=\frac{1}{L}\int_L^{L+2.5}\{P^A(x)(x-3)-[1-P^A(x)](L+3-x)\}dx, \tag{15}$$

$$\frac{\tilde{J}_4}{F}=\frac{1}{L}\int_{L-2.5}^{L}\{P'^A(x)(x-3)-[1-P'^A(x)](L-x+3)\}dx. \tag{16}$$

Simplifying, summing and substituting $L=5$ we obtain the expression for the surface current per particle $\tilde{J}^A/F$ for the case of short terrace length $L=5$,

$$\frac{\tilde{J}^A}{F}=5\tilde{P}^A_{\mathrm{av}}-3, \tag{17}$$

where

$$\tilde{P}^A_{\mathrm{av}}=\frac{\tilde{P}'^A_{\mathrm{up}}+\tilde{P}^A_{\mathrm{up}}}{2} \tag{18}$$

and

$$\tilde{P}'^A_{\mathrm{up}}=\frac{1}{2.5}\int_{2.5}^{5}P'^A(x)dx, \tag{19}$$

$$\tilde{P}^A_{\mathrm{up}}=\frac{1}{2.5}\int_{5}^{7.5}P^A(x)dx. \tag{20}$$

We can see that $L_0=5$ is possible only if $\tilde{P}^A_{\mathrm{av}}=0.6$; for all $0<\tilde{P}^A_{\mathrm{av}}<0.6$, the surface current is negative and the corresponding selected terrace length will be longer than $L_0=5$. Here we note again that geometric DF corresponds to $\tilde{P}^A_{\mathrm{av}}=1/2$ and thus implies a selected terrace length $L_0>5$. For

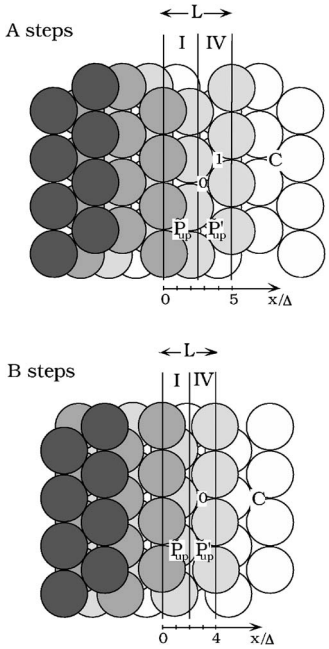

FIG. 4. Schematic diagram (top view) of A and B steps on the fcc(111) surface for the case of short terrace length.

all $\tilde{P}^A_{\rm av} > 0.6$, the surface current is positive and the corresponding selected terrace length will be shorter than $L_0=5$: in between the $L=5$ and the value corresponding to the (100) microfacet ($L=2$), depending on the particular value of $\tilde{P}^A_{\rm av}$ (see Sec. III F 2).

D. Surface current for B steps ($L \geqslant 7$)

The calculation for B steps is similar to that for A steps, except that, as already noted, in this case one has $p=\frac{1}{3}$ and $q=\frac{2}{3}$. The relationship between the absorption site c in the 1D random-walk picture (Fig. 2) and the terrace width L in our units is $L=(3c+8)/2$, where c is an integer, which satisfies $c=2K+2$, where $K=0, 1, 2, 3,\ldots$. In addition, the site closest to the step edge is an fcc site. In this case, the probability for interlayer diffusion from the fcc site is again given by ϵ and the probability of diffusion down the step from the last hcp site on the terrace is given by ϵ', while the γ in Eqs. (3a)–(3c) is given by $\gamma=(2\epsilon+3\epsilon'-2\epsilon\epsilon')/(1+2\epsilon+2\epsilon'-2\epsilon\epsilon')$. Taking all these differences into account, we obtain the following general expression for the total surface current for B steps:

$$\frac{J^B}{F} = \frac{(2-10\epsilon-7\epsilon'+10\epsilon\epsilon')L-24(1-P^B_{\rm av})}{D_B} + \frac{\epsilon[50-6(P'^B_{\rm up}+2P^B_{\rm up})]+\epsilon'(99-24P^B_{\rm av})-\epsilon\epsilon'[50-6(P'^B_{\rm up}+2P^B_{\rm up})]}{D_B}, \quad (21)$$

where $L \geqslant 7$ and $D_B=(4\epsilon+6\epsilon'-4\epsilon\epsilon')L+4-20\epsilon-34\epsilon'+20\epsilon\epsilon'$.

As for A steps, we may use the assumption that the processes of exchange from fcc and hcp sites are basically the same, except for the binding energy difference in order to obtain (see the Appendix) the expressions $\epsilon=\rho/(2+\rho)$ and $\epsilon'=\rho/(3+\rho)$, with $\rho=(\nu_{\rm ES}/\nu_0)\exp(-E^B_{\rm ES}/k_BT)$, where $E^B_{\rm ES}$ corresponds to the Ehrlich-Schwoebel barrier for exchange from the last fcc site and $\nu_{\rm ES}/\nu_0$ is the ratio of prefactors for exchange versus terrace diffusion. Substitution of these expressions into Eq. (21) yields

$$\frac{J^B}{F} = \frac{(4-18\rho-5\rho^2)L-48(1-P^B_{\rm av})+2(38+3P'^B_{\rm up})\rho+25\rho^2}{2[4+2(2L-9)\rho+(L-5)\rho^2]}, \quad (22)$$

where $L \geqslant 7$, along with the corresponding expression for the selected slope

$$m^B_0 = \frac{2\sqrt{2}(4-18\rho-5\rho^2)}{48(1-P^B_{\rm av})-2(38+3P'^B_{\rm up})\rho-25\rho^2} \left(m^B_0 \leqslant \frac{2\sqrt{2}}{7}\right). \quad (23)$$

E. Surface current for B steps ($L=4$)

We now consider the surface current for the special case of shorter terrace lengths $L<7$ for which there is an overlap between regions II and IV and as a result Eqs. (22) and (23) may break down. Since the possible terrace widths for B steps are $L=1, 4, 7,\ldots$, the two possible special cases correspond to $L=1$ and $L=4$. The first case ($L=1$) corresponds to a (111) microfacet, for which the surface current is negative in our model. For the special case $L=4$ we obtain

$$\frac{\tilde{J}^B}{F} = 4\tilde{P}^B_{\rm av} - 3. \quad (24)$$

Here $\tilde{P}^B_{\rm av}=(\tilde{P}'^B_{\rm up}+\tilde{P}^B_{\rm up})/2$, where

$$\tilde{P}^B_{\rm up} = \frac{1}{2}\int_4^6 P^B(x)dx, \quad (25)$$

$$\tilde{P}'^B_{\rm up} = \frac{1}{2}\int_2^4 P'^B(x)dx. \quad (26)$$

We can see that $L_0=4$ is possible only if $\tilde{P}^B_{\rm av}=0.75$; for all $0<\tilde{P}^B_{\rm av}<0.75$, the surface current is negative and corresponding selected terrace length will be longer then $L=4$.

Here we note again that geometric DF corresponds to $\tilde{P}^B_{\rm av}=1/2$ and thus implies a selected terrace length $L_0>4$. For all $\tilde{P}^B_{\rm av}>0.75$, the surface current is positive and the corresponding selected terrace length will be shorter then $L=4$: in between the $L=4$ and the value corresponding to (111) microfacet ($L=1$), depending on the particular value of $\tilde{P}^B_{\rm av}$ (see Sec. III F 2).

F. Calculation of selected slopes for intermediate cases

We note that for certain values of the uphill funneling probabilities, the selected terrace length L_0 will be intermediate between that for a short terrace $[L=5(4)]$ and that for the shortest terrace length that may be considered in general case $[L=8(7)]$ for $A(B)$ steps. Then, the selected slope will be determined by combining our results for the short terrace as described in the previous section with the results corresponding to the general case.

1. Intermediate case 1: $\sqrt{2}/4 \leqslant m_0^A \leqslant 2\sqrt{2}/5$ and $2\sqrt{2}/7 \leqslant m_0^B \leqslant \sqrt{2}/2$

We first consider A steps. We suppose that $\tilde{P}^A_{\rm av}<0.6$ (see Sec. III C) so that the surface current per particle J^A_5/F corresponding to the short terrace $L=5$ is negative. We also assume that the surface current per particle J^A_8/F corresponding to $L=8$ is positive. We are looking for values of N_5 and N_8 such that the total surface current over N_5 terraces of length $L=5$ and N_8 terraces of length $L=8$ is equal to zero

$$8\frac{J^A_8}{F}N_8+5\frac{J^A_5}{F}N_5=0. \tag{27}$$

Here we have taken into account the fact, that the total number of atoms which land on a terrace of width L is proportional to L. The intermediate value of selected slope, corresponding to a mixture of N_5 terraces of length $L=5$ and N_8 terraces of length $L=8$ can then be expressed as

$$m^A_0=\frac{(N_8+N_5)h}{8N_8+5N_5}=\frac{(5-8J^A_8/J^A_5)h}{40(1-J^A_8/J^A_5)}. \tag{28}$$

Using Eq. (13) (with $L=8$) for J^A_8 and Eq. (17) for $\tilde{J}^A=J^A_5$ with $h=2\sqrt{2}$, we obtain

$$m^A_0=\frac{-\sqrt{2}[12-576P^A_{\rm av}+170\rho-72P'^A_{\rm up}\rho+41\rho^2+75\tilde{P}^A_{\rm av}(4+14\rho+3\rho^2)]}{20[12+72P^A_{\rm av}+26\rho+9P'^A_{\rm up}\rho+5\rho^2-15\tilde{P}^A_{\rm av}(4+14\rho+3\rho^2)]}. \tag{29}$$

Using the same approach, we can obtain the intermediate value of selected slope corresponding to a mixture of terraces with terrace lengths $L=4$ and $L=7$ for B steps

$$m^B_0=\frac{-\sqrt{2}[22-168P^B_{\rm av}+55\rho-21P'^B_{\rm up}\rho+11\rho^2+32\tilde{P}^B_{\rm av}(2+5\rho+\rho^2)]}{14[2+24P^B_{\rm av}+5\rho+3P'^B_{\rm up}\rho+\rho^2-8\tilde{P}^B_{\rm av}(2+5\rho+\rho^2)]}. \tag{30}$$

2. Intermediate case 2: mixture of short terraces and facets

For higher values of the uphill funneling probabilities, such that the surface current is positive for short terraces, the selected terrace length will be intermediate between that for a microfacet ($L=2$ for A steps and $L=1$ for B steps) and the short terrace ($L=5$ for A steps and $L=4$ for B steps), e.g. $2\sqrt{2}/5 \leqslant m^A_0 \leqslant \sqrt{2}$ and $\sqrt{2}/2 \leqslant m^B_0 \leqslant 2\sqrt{2}$. We first consider the case of A-steps ($\tilde{P}^A_{av}>0.6$, see Sec. III C). We assume that there are n^f regions with N^f_i microfacets in each region, where $1 \leqslant i \leqslant n^f$ and, similarly, there are n^t regions with N^t_i terraces in each region, where $1 \leqslant i \leqslant n^t$. The total number of facets is $N^f=\Sigma_{i=1}^{n^f}N^f_i$ and the total number of terraces is $N^t=\Sigma_{i=1}^{n^t}N^t_i$. Once the values of N^f and N^t are determined, the mound slope may be expressed as

$$\langle m^A\rangle=\frac{N^t+N^f}{5N^t+2N^f}h, \tag{31}$$

where $h=2\sqrt{2}$.

Without loss of generality we can assume that $n^f=n^t=n$. The surface current per particle corresponding to a region composed of a sequence of N^f_i microfacets can be expressed as (see Fig. 5)

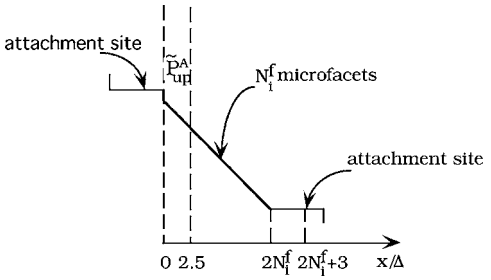

FIG. 5. Details of facetted region composed of N^f_i microfacets.

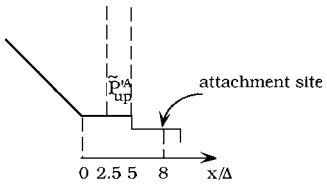

FIG. 6. Details of deposition over the topmost terrace in a sequence of short terraces.

$$\frac{J_i^f}{F} = \frac{1}{L}\int_0^{2.5} \{P^A(x)(2+x) - [1-P^A(x)](2N_i^f + 3 - x)\}dx - \frac{1}{L}\int_{2.5}^{2N_i^f} [2N_i^f + (3-x)]dx, \tag{32}$$

where $L=2N^f+5N^t$ and we assume that any particle deposited on a facet diffuses to the attachment site at the lower terrace. This may be rewritten as

$$\frac{J_i^f}{F} = \frac{1}{L}[12.5\tilde{P}^A_{\rm up} + 5\tilde{P}^A_{\rm up}N_i^f - 6N_i^f - 2(N_i^f)^2], \tag{33}$$

where

$$\tilde{P}^A_{\rm up} = \frac{1}{2.5}\int_5^{7.5} P^A(x)dx. \tag{34}$$

The total contribution to the surface current per particle due to the facetted regions can be expressed as

$$\frac{J^f}{F} = \sum_{i=1}^{n}\frac{J_i^f}{F} = \frac{1}{L}\left[12.5\tilde{P}^A_{\rm up}n - (6-5\tilde{P}^A_{\rm up})N^f - 2\sum_{i=1}^{n}(N_i^f)^2\right]. \tag{35}$$

We now consider the surface current due to the regions composed of short terraces, which include three contributions: J_1 due to the topmost terrace in each region (Fig. 6), J_2 due to the bottom terrace in each region (Fig. 7), and J_3 due to the interior terraces in each region. The surface current J_3 may be calculated using the general expression for the surface current of the short terrace. However, to calculate J_1 and J_2 one must take into account the effect of the neighboring facet.

The current J_1 may be written as

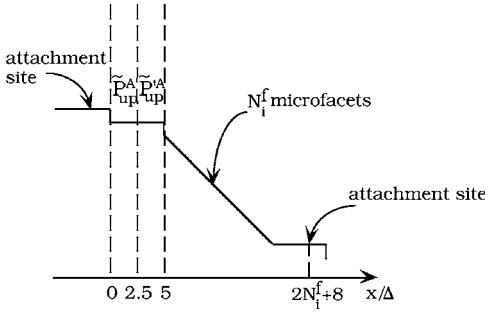

FIG. 7. Details of deposition over the bottom terrace in a sequence of short terraces.

$$\frac{J_1^t}{F} = \frac{n}{L}\int_0^{2.5}(x-3)dx + \frac{n}{L}\int_{2.5}^{5}\{P'^A(x)(x-3) - [1-P'^A(x)](8-x)\}dx = \frac{n}{L}[12.5\tilde{P}'^A_{\rm up} - 15], \tag{36}$$

where

$$\tilde{P}'^A_{\rm up} \equiv \frac{1}{2.5}\int_{2.5}^{5} P'^A(x)dx. \tag{37}$$

The current J_2 may be written

$$\frac{J_2^t}{F} = \frac{1}{L}\sum_{i=1}^{n}\left[\int_0^{2.5}\{P^A(x)(2+x) - [1-P^A(x)](3-x)\}dx + \int_{2.5}^{5}\{P'^A(x)(x-3) - [1-P'^A(x)](2N_i^f + 8 - x)\}dx\right], \tag{38}$$

where the factor N_i^f takes into account the probability that an atom deposited near the step edge lands on the facet and diffuses to the bottom of the facetted region:

$$\frac{J_2^t}{F} = \frac{1}{L}[25\tilde{P}^A_{\rm av}n - 15n - 5(1-\tilde{P}'^A_{\rm up})N^f]. \tag{39}$$

Using Eq. (17) for the surface current per particle due to a single terrace, the contribution from all the other terraces can be expressed as

$$\frac{J_3^t}{F} = \frac{\tilde{J}^A}{F}\frac{5(N^t-2n)}{L} = \frac{5}{L}(5\tilde{P}^A_{\rm av} - 3)(N^t - 2n), \tag{40}$$

where the factor of N^t-2n corresponds to the total number of short terraces in this intermediate region. Combining all three contributions and using the simplifying assumption that $N_i^f=N^f$ and $N_i^t=N^t$ for all i, along with the requirement that the total surface current is zero, yields

$$(N^f)^2 + (11-10\tilde{P}^A_{\rm av})N^f + 5(3-5\tilde{P}^A_{\rm av})N^t = 0. \tag{41}$$

Solving for N^f, we obtain for A steps

$$N^f = \frac{-(11-10\tilde{P}^A_{\rm av}) + \sqrt{(11-10\tilde{P}^A_{\rm av})^2 - 40(3-5\tilde{P}^A_{\rm av})N^t}}{4}, \quad (0.6 < \tilde{P}^A_{\rm av} \leqslant 1). \tag{42}$$

For simplicity we have made the reasonable assumption that the uphill funneling probability for atoms deposited above the facetted region adjacent to the upper terrace within a distance $\delta=2.5$ from the step edge has the same distribution $P^A(x)$ $[P'^A(x)]$ as in the case of the deposition near step-edge between two short terraces (see Sec. III A).

Using the same approach, we can obtain the intermediate value of the selected slope corresponding to a mixture of short terraces ($L=4$) and (111) microfacets ($L=1$) for B steps

$$\langle m^B \rangle = \frac{N^t + N^f}{4N^t + N^f} h, \tag{43}$$

where again $h=2\sqrt{2}$ and

$$N^f = \frac{-2(5-4\tilde{P}^B_{\rm av}) + \sqrt{4(5-4\tilde{P}^B_{\rm av})^2 + 32(4\tilde{P}^B_{\rm av}-3)N^t}}{2}, \tag{44}$$

$$(0.75 < \tilde{P}^B_{\rm av} \leqslant 1).$$

We note that Eqs. (31) and (42)–(44) indicate that the selected slope depends on the values of N_t. However, for realistic values of uphill funneling probabilities, we find that, except for small N_t, this dependence is relatively weak.

IV. DISCUSSION

Our results indicate that there are two key parameters which determine the surface current and selected mound slope. The first parameter $\rho=(\nu_{\rm ES}/\nu_0)\exp(-E_{\rm ES}/k_BT)$ corresponds to the Ehrlich-Schwoebel barrier and is typically different for A and B steps. The second set of parameters $P'_{\rm up}$ and $P_{\rm up}$ corresponds to the interaction of a depositing atom with a step edge, and as recent molecular dynamics simulations have shown,[26] can also be very different for A and B steps. We note that for the case of an infinite ES barrier corresponding to $\rho=0$, our general expressions for the selected slope [Eq. (14) and Eq. (23) for A and B steps, respectively] reproduce the results previously derived for this case[26] which are valid when the selected slope is not too high, i.e.,

$$m_0 = \frac{\sqrt{2}}{6(1-P_{\rm av})}, \quad m_0 < m_c, \tag{45}$$

where $P_{\rm av}=(P_{\rm up}+P'_{\rm up})/2$ and $m_c=\sqrt{2}/4$ $(2\sqrt{2}/7)$ for A (B) steps. We now discuss in more detail our results for the case of a finite ES barrier $(\rho \neq 0)$.

We first note that Eqs. (13), (14), (22), and (23) for the surface current and mound slopes for A and B steps can be written in the following general form:

$$\frac{J}{F} = \frac{(A - B\rho - C\rho^2)L - (D - E\rho - F\rho^2)}{X}, \tag{46}$$

$$m_0 = \frac{A - B\rho - C\rho^2}{D - E\rho - F\rho^2}, \tag{47}$$

where the constants $A,B,C,D,E,F>0$ and the denominator $X>0$ for all terrace widths L for which they are valid. Since the criterion for a mound instability is that the surface current is positive for small slopes, while the selected slope m_0 is determined by the zero of the surface current, this implies that there exists a critical value $\rho=\rho_c$, corresponding to the positive root of the numerator of Eq. (47), e.g., $A-B\rho-C\rho^2=0$. Since the numerators in Eqs. (14) and (23) are independent of the uphill funneling probabilities, the critical value of ρ is also independent, i.e.,

$$\rho_c = \frac{-9+\sqrt{101}}{5} \simeq 0.21 \tag{48}$$

for both A and B steps. For $\rho<\rho_c$ the surface is unstable to mound formation since the surface current is positive for small slopes (large L). In contrast, for $\rho>\rho_c$ there is no mound instability for small slopes. We note that similar behavior in which the critical ES barrier for mound formation is independent of the upward funneling probability has previously been observed in calculations of surface current and selected slope for the case of irreversible growth on (100) metal surfaces.[16,17]

We may also define ρ_0 as the positive root of the denominator of Eq. (47), e.g., $D-E\rho-F\rho^2=0$. Using Eqs. (13) and (22) we obtain

$$\rho_0^A = \frac{1}{76}[(-116 - 9P'^A_{\rm up}) + \sqrt{24400 - 10944P^A_{\rm av} + 2088P'^A_{\rm up} + 81(P'^A_{\rm up})^2}], \tag{49a}$$

$$\rho_0^B = \frac{1}{50}[-2(38+3P'^B_{\rm up}) + \sqrt{4800(1-P^B_{\rm av}) + 4(38+3P'^B_{\rm up})^2}]. \tag{49b}$$

Depending on the values of $P_{\rm av}$ and $P'_{\rm up}$, there are then two different possible scenarios for the dependence of the selected mound slope on the parameter ρ.

Scenario 1: $\rho_c \leqslant \rho_0$. This scenario applies when the uphill funneling probabilities $P_{\rm up}$ and $P'_{\rm up}$ are not too high. For example, the usual downward funneling assumption[21,22] $(P_{\rm up}=0,\ P'_{\rm up}=1,\ P_{\rm av}=1/2)$ falls into this scenario. Scenario 1 may be further divided into two cases.

(a) Surface current is negative for short terraces [$\tilde{P}^A_{\rm av} < 0.6$ for A steps and $\tilde{P}^B_{\rm av} < 0.75$ for B steps (see Sec. III C)]. In this case, as ρ approaches the critical value ρ_c from below, the selected mound slope decreases continuously to zero [see Fig. 8(a)]. However, for $\rho>\rho_c$, the surface current is negative for all slopes and there is no instability.

(b) Surface current is positive for short terraces [$\tilde{P}^A_{\rm av} > 0.6$ for A steps and $\tilde{P}^B_{\rm av} > 0.75$ for B steps (see Sec. III C)].

In this case the behavior of the selected slope is similar to (a) for small slopes and ρ slightly less than ρ_c. However, for small ρ the selected slope corresponds to a mixture of short terraces and facets and is typically independent of ρ. In addition, for $\rho>\rho_c$, while the surface current is negative for small slopes, for $m>m^*(\rho)$ (where $m^*(\rho)$ may be calculated for A steps (B steps) using Eqs. (29) and (30)—see dashed curves in Figs. 9(b) and 11(b)) it becomes positive due to the contribution from short terraces. As a result, if a fluctuation, due for example to deposition noise, leads to a local slope $m_{\rm loc}>m^*(\rho)$, then fluctuation-induced mound formation will occur with a selected slope which is the same as for small ρ. Such a fluctuation-induced instability may occur even for a small or negative ES barrier.

Scenario 2: $\rho_c > \rho_0$. This scenario applies when the uphill funneling probabilities $P_{\rm up}$ and $P'_{\rm up}$ are relatively high. As ρ

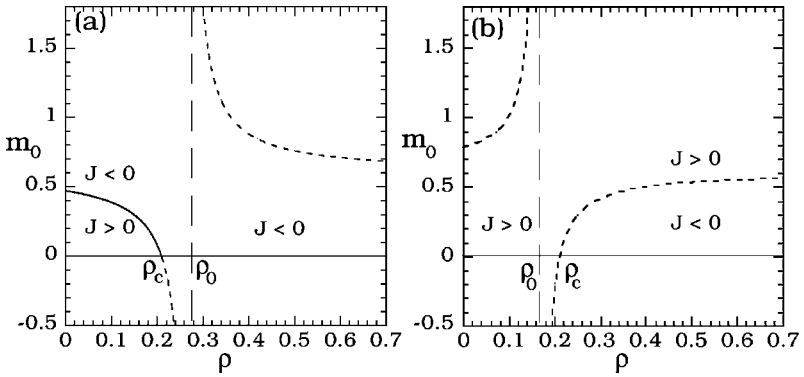

FIG. 8. (a) Corresponds to scenario 1 and (b) corresponds to scenario 2. The solid curve indicates the branch which includes valid general solutions, while dashed curves correspond to general solutions which are either outside the valid range or do not correspond to an instability (see text).

increases, the general expression for the selected slope (47) diverges at $\rho=\rho_0$ [see Fig. 8(b)]. In addition for $\rho_0<\rho<\rho_c$, the general expression predicts a negative selected slope. As a result, the values of the selected slope predicted by the general Eqs. (14) and (23) for $0\leq\rho<\rho_c$ are outside the limits of their validity, e.g., $m_0^A<\sqrt{2}/4\simeq 0.35$ and $m_0^B<2\sqrt{2}/7\simeq 0.40$ which correspond to the minimum terrace lengths that may be considered in our general calculations of the surface current and selected mound slope. Accordingly, the selected slopes need to be calculated by considering the special cases corresponding to either a mixture of short terraces and the shortest terraces that may be considered in the general case (Sec. III F 1), or of facets and short terraces (Sec. III F 2). In contrast while the surface is stable for small slopes for $\rho>\rho_c$, due to the large uphill funneling probabilities the surface becomes again unstable for large slopes $m>m^*(\rho)$. As for the case of scenario 1(b) this leads to the possibility of fluctuation-induced mound formation for large ρ (small ES barrier).

Figures 9–12 show the range of possible behaviors for the selected slope as a function of ρ for both scenarios for A and B steps. We note that while results are shown for $\rho<1$ corresponding to $E_{\mathrm{ES}}>0$, the fluctuation-induced instability regime also extends to $\rho>1$ corresponding to a negative ES barrier. The results shown correspond to values of P_{av} ranging from zero (maximum downhill funneling) to very strong uphill funneling (P_{av} close to 1). As shown in Figs. 9(a) and 11(a), for small uphill funneling the first scenario holds for both A and B steps. In particular, for $\rho>\rho_c$ the surface is stable, while for $\rho<\rho_c$ the mound slope decreases with increasing ρ. In addition, as the uphill funneling probability increases, the selected mound slope m_0 increases more rapidly with decreasing ρ. In contrast, Figs. 9(b) and 11(b) correspond to case (b) of the first scenario when the uphill funneling is not too large, but large enough so that the surface current is positive on the "short" terraces ($\tilde{P}_{\mathrm{av}}^A>0.6$ for A steps and $\tilde{P}_{\mathrm{av}}^B>0.75$ for B steps—see Sec. III C). As can be seen, the selected slope is large and constant for small ρ and decreases for intermediate ρ ($\rho<\rho_c$). For $\rho>\rho_c$ there is no instability for small slopes. However, for large enough slopes a fluctuation-induced instability is possible.

In contrast, for larger uphill funneling, the second scenario holds as shown in Figs. 10 and 12. In this case the selected mound slope corresponds to a mixture of facets and short terraces and depends on the uphill funneling probability, but does not depend on ρ for $\rho<\rho_c$. For $\rho>\rho_c$ the surface is stable to small fluctuations in the slope. However, for slopes $m>m^*(\rho)$ there is an instability and the value of the selected slope (dashed horizontal lines in Figs. 10 and 12) corresponds to a mixture of facets and short terraces, just as for $\rho<\rho_c$.

We note that in recent molecular dynamics simulations of deposition near steps on fcc(111) metal surfaces,[26] the uphill funneling probabilities were found to be much stronger for A steps than for B steps, due to the differences in step geometry. In particular it was found that for A steps, due to the short-range attraction of depositing atoms to the step-edge, the overall uphill funneling probability P_{av}^A is significantly larger than predicted by downward funneling. This corresponds to the second scenario (see Fig. 10). In particular, the parameters used in Fig. 10 correspond to the uphill funneling values obtained in molecular dynamics simulations of deposition at Ag(111) A steps[26] along with an estimate for $\tilde{P}_{\mathrm{av}}^A$ for short terraces. In contrast, due to the high probability of "knockout" or exchange at B steps, the overall uphill funneling probability P_{av}^B is significantly lower which leads to the

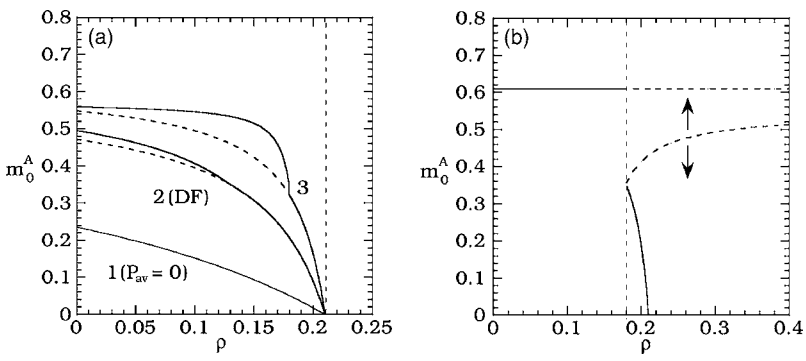

FIG. 9. Selected mound slope of A steps as function of ρ (scenario 1) for several different values of P_{av} and $\tilde{P}_{\mathrm{av}}$. (a) P_{av} and $\tilde{P}_{\mathrm{av}}$ are not too large ($\tilde{P}_{\mathrm{av}}<0.6$). Case 1 corresponds to $P_{\mathrm{av}}=0$, case 2 to $P_{\mathrm{av}}=1/2$ (DF), case 3 to $P_{\mathrm{av}}=0.57$, $\tilde{P}_{\mathrm{av}}=0.59$. (b) Discontinuity in slope ($P_{\mathrm{av}}=0.57$, $P'_{\mathrm{up}}=1$, $\tilde{P}_{\mathrm{av}}=0.65$). The dashed curve indicates critical slope for fluctuation-induced mound formation.

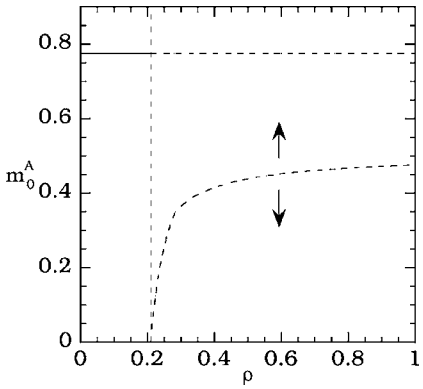

FIG. 10. Selected mound slope of A steps as function of ρ for scenario 2 (enhanced uphill funneling). Parameters here are $P_{\mathrm{av}}=0.72$, $\tilde{P}_{\mathrm{av}}=0.76$, $P'_{\mathrm{up}}=1$. Dashed curve indicates critical slope for fluctuation-induced mound formation.

first scenario. In particular, case 3 of Fig. 11(a) corresponds to the uphill funneling values obtained in molecular dynamics simulations of deposition at Ag(111) B steps[26] along with an estimate for $\tilde{P}^B_{\mathrm{av}}$ for short terraces. We note that these results imply a significant mound-slope anisotropy in agreement with the scanning-tunneling microscopy pictures of the large-scale mounds formed during room-temperature growth of Ag/Ag(111).[2]

V. CONCLUSIONS

We have obtained general expressions for the surface current and selected mound slope for irreversible growth on a regular stepped fcc(111) surface with two types of close-packed step edges (A and B steps). In our calculations we have taken into account the effects of the interaction between depositing atoms and steps, as well as the effects of a finite ES barrier to interlayer diffusion of atoms at the last fcc and hcp sites near the step edge. The resulting expressions for the surface current and selected mound slope depend sensitively on the values of the uphill funneling probabilities as well as on the value of the parameter $\rho=(\nu_{\mathrm{ES}}/\nu_0)\exp(-E_{\mathrm{ES}}/k_BT)$.

In our calculations we have also considered the case of short terrace lengths ($L=4$ for B steps and $L=5$ for A steps) for which our general expressions for the surface current and selected mound slope may break down. In particular, it was shown that for enhanced uphill funneling with $\tilde{P}_{\mathrm{av}}>\tilde{P}^c_{\mathrm{av}}$

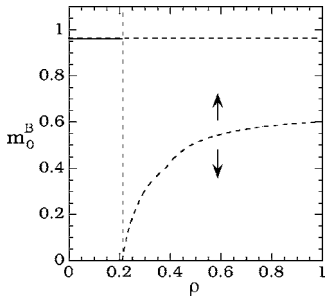

FIG. 12. Selected mound slope of B steps as function of ρ for scenario 2 (enhanced uphill funneling). Parameters here are $P_{\mathrm{av}}=0.8$, $\tilde{P}_{\mathrm{av}}=0.9$, $P'_{\mathrm{up}}=1$. Dashed curve indicates critical slope for fluctuation-induced mound formation.

(where $\tilde{P}^c_{\mathrm{av}}=0.6$ for A steps and $\tilde{P}^c_{\mathrm{av}}=0.75$ for B steps) short terraces must be considered when calculating the selected mound slope. In particular, we have considered the case when the slope is intermediate between that corresponding to the shortest possible terrace in the general case ($L^B=7$ and $L^A=8$) and the "short" terrace ($L^B=4$ and $L^A=5$) corresponding to a terrace with one empty row of fcc adsorption sites, e.g., $\sqrt{2}/4\leqslant m_0^A\leqslant 2\sqrt{2}/5$ and $2\sqrt{2}/7\leqslant m_0^B\leqslant\sqrt{2}/2$. We have also considered the case when the slope is even larger and is intermediate between that corresponding to a "short" terrace and a facet [(111) microfacet for B steps or (100) microfacet for A steps]. We note that in our calculations we assumed perfect "downward funneling" for atoms deposited on microfacets. While this is a reasonable approximation for short microfacets, for larger microfacets it is more suitable for B steps than for A steps due to the low activation energies for diffusion on (111) microfacets. Consideration of this effect is likely to lead to a further enhancement of the anisotropy already observed in our calculations.

We have also analyzed the expressions for the surface current and selected mound slope and discussed two possible scenarios corresponding to different values of the key parameters. In particular, we found that the critical value of ρ, e.g., $\rho_c=(-9+\sqrt{101})/5\simeq 0.21$ is independent of the degree of uphill funneling. In both scenarios the surface is unstable for $\rho<\rho_c$ for small slopes while for $\rho>\rho_c$ the surface is stable for small slopes. For small values of uphill funneling, scenario 1 holds and the selected slope decreases with increasing ρ up to the value $\rho=\rho_c$, while for $\rho>\rho_c$ there is no instability. However, for larger values of uphill funneling

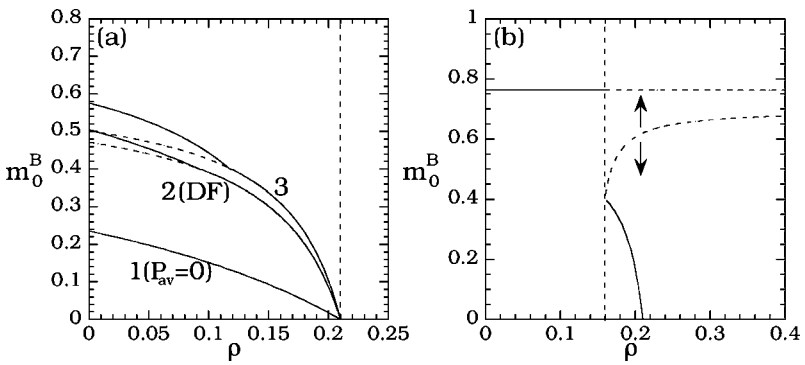

FIG. 11. Selected mound slope of B steps as function of ρ (scenario 1) for several different values of P_{av} and $\tilde{P}_{\mathrm{av}}$. (a) P_{av} and $\tilde{P}_{\mathrm{av}}$ both not too large ($\tilde{P}_{\mathrm{av}}<0.75$). Case 1 corresponds to $P_{\mathrm{av}}=0$, case 2 to $P_{\mathrm{av}}=1/2$ (DF), case 3 to $P_{\mathrm{av}}=0.53$, $P'_{\mathrm{up}}=0.71$, $\tilde{P}_{\mathrm{av}}=0.62$. (b) Discontinuity in slope ($P_{\mathrm{av}}=0.57$, $P'_{\mathrm{up}}=0.9$, $\tilde{P}_{\mathrm{av}}=0.77$). Dashed curve indicates critical slope for fluctuation-induced mound formation.

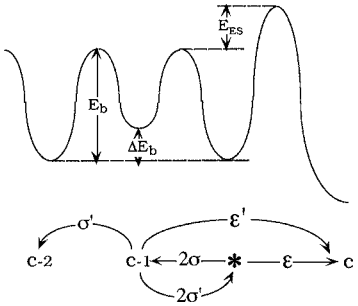

FIG. 13. Diagram showing details of diffusion down the step for B steps.

probabilities, e.g., $\tilde{P}_{\mathrm{av}} > 0.6$ (0.75) for A steps (B steps), the surface may become unstable even for $\rho > \rho_c$ and the selected slope may reach the value corresponding to the mixture of facets and short terraces. Thus, in this case there exists the possibility of mound formation due to fluctuations even for a small ES barrier. We note such a fluctuation-induced instability is a new phenomenon which has not been previously discussed. Similar behavior is observed for the case of even larger values of the uphill funneling probabilities such that scenario 2 holds. In this case the selected slope corresponds to a mixture of facets and short terraces and is approximately constant for $\rho < \rho_c$. However, for $\rho > \rho_c$, the surface again becomes unstable for larger slopes. Thus, in this case there again exists the possibility of mound formation due to fluctuations even for a small ES barrier.

Finally, we note that while our model is as general as we could make it, it is possible that for some metal (111) surfaces a more complicated model would be required. For example, it has recently been suggested[27] that in some (111) systems correlated jumps may play an important role in the diffusion process. While it is unclear how this would affect the surface current, we note that this effect is mainly important at higher temperatures. We also note that field-ion-microscope studies of diffusion on Ir(111) (Refs. 31 and 32) indicate that the potential energy surface for an atom near a step edge may include the existence of a so called "empty zone" separating the central region of the terrace from the step-edge region. For such systems, our model would have to be modified to take this into account.

ACKNOWLEDGMENTS

We would like to acknowledge support from a type AC grant from the Petroleum Research Fund and from the NSF through Grant No. DMR-0219328.

APPENDIX: CALCULATION OF $\gamma(\rho)$

Here we first obtain a general expression for γ as a function of the probabilities ϵ and ϵ' of diffusion down a step from the fcc and hcp sites closest to the step edge. Using reasonable assumptions about the exchange process and symmetry of the saddle-point site, this leads to a direct expression for γ as a function of the Erhlich-Schwoebel parameter ρ. We first consider the case of B steps. In this case (see Figs. 2, 3, and 13) one may write

$$P_{c-1} = \sigma' P_{c-2} + 2\sigma' P_*, \tag{A1}$$

$$P_* = 2\sigma P_{c-1}, \tag{A2}$$

where $\sigma' = (1-\epsilon')/3$ is the probability of going from the last hcp site at the edge of the terrace to any of the three nearby fcc sites and $\sigma = (1-\epsilon)/2$ is the probability of going from the last fcc site at the edge of the terrace to any of the two nearby hcp sites. P_i is the probability that a particle deposited at site i will be absorbed at site 0. P_* corresponds to the last site on the terrace, which is an fcc site in case of B steps. Solving we obtain

$$P_{c-1} = \frac{\sigma'}{1-4\sigma\sigma'} P_{c-2}. \tag{A3}$$

Comparing with Eq. (1c) that defines γ, e.g., $P_{c-1} = (1-\gamma)P_{c-2}$ and substituting for σ and σ' we obtain

$$\gamma = \frac{2\epsilon + 3\epsilon' - 2\epsilon\epsilon'}{1 + 2\epsilon + 2\epsilon' - 2\epsilon\epsilon'}. \tag{A4}$$

We now assume that the rate for hopping from the last fcc site (*) to any of the one of the two nearby hcp sites $(c-1)$ is given by $D = \nu_0 e^{-E_d/k_B T}$(where E_a is the corresponding activation energy for diffusion from fcc to hcp sites on the flat terrace) while the rate for interlayer diffusion from the last hcp site $(c-1)$ is given by $D_{\mathrm{ES}} = \nu_{\mathrm{ES}} e^{-(E_a + E_{\mathrm{ES}})/k_B T}$. We thus obtain

$$\sigma = \frac{D}{2D + D_{\mathrm{ES}}} = \frac{1}{2+\rho}, \tag{A5}$$

where $\rho = D_{\mathrm{ES}}/D = (\nu_{\mathrm{ES}}/\nu_0) e^{-E_{\mathrm{ES}}/k_B T}$.

We now assume that the saddle-points for interlayer exchange from the last hcp site and the last fcc site are essentially the same (see Ref. 28). Defining the difference between the binding energies of adatoms at fcc and hcp sites as $\delta E_b = E_b^{\mathrm{fcc}} - E_b^{\mathrm{hcp}}$, we can see that the rate for hopping from the last hcp site $(c-1)$ to any of the nearby fcc sites is given by $D' = e^{\delta E_b/k_B T} D$ while the rate for interlayer diffusion from the last hcp site $(c-1)$ is given by $D'_{\mathrm{ES}} = e^{\delta E_b/k_B T} D_{\mathrm{ES}}$. Thus we obtain for σ',

$$\sigma' = \frac{D'}{3D' + D'_{\mathrm{ES}}} = \frac{D}{3D + D_{\mathrm{ES}}} = \frac{1}{3+\rho}. \tag{A6}$$

Solving for ϵ and ϵ' we obtain $\epsilon = 1 - 2\sigma = \rho/(2+\rho)$ and $\epsilon' = 1 - 3\sigma = \rho/(3+\rho)$. Substituting in Eq. (A4) we obtain

$$\gamma(\rho) = \frac{\rho(4+\rho)}{2 + 5\rho + \rho^2}. \tag{A7}$$

For A steps we can use the same approach, except that the last site on the terrace is an hcp site. In this case we obtain $\gamma = (3\epsilon + 2\epsilon' - 2\epsilon\epsilon')/(1 + 2\epsilon + 2\epsilon' - 2\epsilon\epsilon')$, where now $\epsilon = \rho/(3+\rho)$ and $\epsilon' = \rho/(2+\rho)$. This again leads to Eq. (A7) for A steps, although in general the values of E_{ES} and thus ρ are different for A and B steps.

*Electronic address: vborovi@physics.utoledo.edu
†Electronic address: jamar@physics.utoledo.edu

[1] Z. Zhang and M. G. Lagally, Science **276**, 377 (1997).
[2] J. Vrijmoeth, H. A. van der Vegt, J. A. Meyer, E. Vlieg, and R. J. Behm, Phys. Rev. Lett. **72**, 3843 (1994).
[3] W. C. Elliott, P. F. Miceli, T. Tse, and P. W. Stephens, Phys. Rev. B **54**, 17 938 (1996).
[4] W. C. Elliott, P. F. Miceli, T. Tse, and P. W. Stephens, Physica B **221**, 96 (1996).
[5] W. C. Elliott, P. F. Miceli, T. Tse, and P. W. Stephens, in *Surface Diffusion: Atomistic and Collective Processes*, Proceedings of the NATO-ASI Series B: Physics (1996).
[6] J. Alvarez, E. Lundgren, X. Torrelles, and S. Ferrer, Phys. Rev. B **57**, 6325 (1998).
[7] C. E. Botez, P. F. Miceli, and P. W. Stephens, Phys. Rev. B **64**, 125427 (2001).
[8] C. E. Botez, W. C. Elliott, P. F. Miceli, and P. W. Stephens, Mater. Res. Soc. Symp. Proc. **672**, O1.5 (2001).
[9] C. E. Botez, W. C. Eliott, P. F. Miceli, and P. W. Stephens, Mater. Res. Soc. Symp. Proc. **672**, O2.7(2001).
[10] N.-E. Lee, D. G. Cahill, and J. E. Greene, Phys. Rev. B **53**, 7876 (1996).
[11] S. J. Chey, J. E. Van Nostrand, and D. G. Cahill, Phys. Rev. Lett. **76**, 3995 (1996).
[12] J. E. Van Nostrand, S. J. Chey, and D. G. Cahill, Phys. Rev. B **57**, 12 536 (1998).
[13] B. W. Karr, D. G. Cahill, I. Petrov, and J. E. Greene, Phys. Rev. B **61**, 16 137 (2000).
[14] A. Raviswaran and D. G. Cahill, Phys. Rev. B **69**, 165313 (2004).
[15] S. C. Wang and G. Ehrlich, Phys. Rev. Lett. **70**, 41 (1993).
[16] J. G. Amar and F. Family, Phys. Rev. B **54**, 14 071 (1996).
[17] J. G. Amar and F. Family, Phys. Rev. Lett. **77**, 4584 (1996).
[18] M. V. R. Murty and B. H. Cooper, Phys. Rev. Lett. **83**, 352 (1999).
[19] G. Ehrlich and F. Hudda, J. Chem. Phys. **44**, 1039 (1966).
[20] R. L. Schwoebl, J. Appl. Phys. **40**, 614 (1969).
[21] J. W. Evans, D. E. Sanders, P. A. Thiel, and A. E. DePristo, Phys. Rev. B **41**, 5410 (1990).
[22] H. C. Kang and J. W. Evans, Surf. Sci. **271**, 321 (1992).
[23] M. Siegert and M. Plischke, Phys. Rev. Lett. **73**, 1517 (1994).
[24] M. Siegert and M. Plischke, Phys. Rev. E **53**, 307 (1996).
[25] J. Yu and J. G. Amar, Phys. Rev. Lett. **89**, 286103 (2002).
[26] J. Yu and J. G. Amar, Phys. Rev. B **69**, 045426 (2004).
[27] J. Ferron, L. Gomez, J. J. de Miguel, and R. Miranda, Phys. Rev. Lett. **93**, 166107 (2004).
[28] P. J. Feibelman, Phys. Rev. Lett. **81**, 168 (1998).
[29] D. D. Vvedensky, A. Zangwill, C. N. Luse, and M. R. Wilby, Phys. Rev. E **48**, 852 (1993).
[30] J. Yu, Ph.D. thesis, University of Toledo, Toledo, 2003.
[31] T.-Y. Fu, H.-T. Wu, and T. T. Tsong, Phys. Rev. B **58**, 2340 (1998).
[32] S.-M. Oh, K. Kyuno, S. C. Wang, and G. Ehrlich, Phys. Rev. B **67**, 075413 (2003).
[33] Here we assume that the diffusion length l_D is sufficiently large, compared to the terrace length l. However, when $l_D \leqslant l$, the surface current may be modified by the presence of the islands nucleating on the terrace.